World Academy of Science, Engineering and Technology
International Journal of Biomedical and Biological Engineering
Vol:7, No:11, 2013

Theoretical Analysis of a Crossed-Electrode 2D Array for 3D Imaging

Yuriy Tasinkevych, Eugene Danicki

Open Science Index, Biomedical and Biological Engineering Vol:7, No:11, 2013 publications.waset.org/17328/pdf

***Abstract*—**Planar systems of electrodes arranged on both sides of dielectric piezoelectric layer are applied in numerous transducers. They are capable of electronic beam-steering of generated wave both in azimuth and elevation. The wave-beam control is achieved by addressable driving of two-dimensional transducer through proper voltage supply of electrodes on opposite surfaces of the layer. In this paper a semi-analytical method of analysis of the considered transducer is proposed, which is a generalization of the well-known BIS-expansion method. It was earlier exploited with great success in the theory of interdigital transducers of surface acoustic waves, theory of elastic wave scattering by cracks and certain advanced electrostatic problems. The corresponding nontrivial electrostatic problem is formulated and solved numerically.

***Keywords*—**Beamforming, transducer array, BIS-expansion.

I. Introduction

RECENTLY there has been a high demand for two-dimensional (2-D) transducer arrays for medical ultrasonography. In the case of ultrasound imaging (e.g. B-mode) using a linear transducer array the 2-D cross-section slices are obtained. Mechanical steering in the elevation direction can be used to combine these cross-sectional slices to achieve volumetric imaging. To accomplish completely electronic focusing and high-speed volumetric scanning the 2-D matrix of piezoelectric transducers were developed and implemented recently. Introducing the second dimension in the array of transducers allows to perform electronic steering in elevation (in contrast to the mechanical steering mentioned above in the case of 1-D arrays) and reduce the slice thickness, resulting in better volumetric imaging quality and resolution [1]. This offers potentialities for developing of the 3-D ultrasound imaging. This new modality overcomes limitations of 2D viewing of 3-D anatomy, using conventional ultrasound techniques. In contrast to 2-D case, where the sequence of 2D images is transformed by the operator in his mind to obtain the impression of 3-D viewing, in 3-D ultrasound imaging this activity is performed by the computer. This leads to more efficient and faster examination, diagnostic and monitoring of therapeutic procedures free of potential inaccuracies related to subjective operator dependent treatment.

To achieve high imaging quality and faultless work of medical 3-D scanners, the corresponding 2-D matrix of transducers must be carefully designed including the array fabrication, the electronic integration and the device packaging. And a matter of great importance is developing corresponding analytical and numerical models of 2-D array transducers in order to perform its accurate analysis and performance verification prior to fabrication. Several 2-D planar phase-array transducer configurations have been proposed for medical diagnostics [2], [3]. Among them the classical design is the square or matrix architecture [4] (see Fig. 1). The typical geometry of a 2-D transducer array is illustrated in Fig. 1.

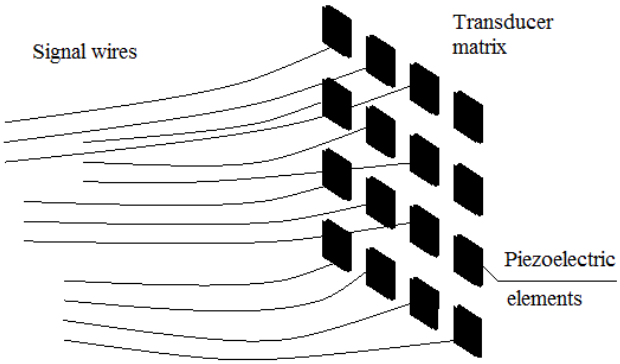


Fig. 1 Typical 2D array of piezoelectric transducers with signal wires

As seen from Fig. 1 fabrication of a typical square 2-D array transducer requires a large number of signal wires to be connected to individual piezoelectric elements which introduces considerable technological difficulties, such as increased costs and complexity of electronic drive circuits wiring, especially at higher operating frequencies [5]. For instance given 256×256 matrix there are above 65e3 signal channels with typical dimensions ~$\lambda/2$ in water so that each 5 MHz array element is 0.15×0.15. To alleviate these problems recently in the literature conceptually different 2-D transducer array architecture has been considered. Specifically, a 2-D structure of an edge-connected, crossed-electrode array was considered in [6], [7]. A sketch showing the electrode patterns arranged on both sides of piezoelectric layer is illustrated in Fig. 2. The proposed transducer is capable of control $N \times M$ elements with $N+M$ signal channels. However no profound theoretical analysis of the considered crossed-electrode array has been carried out so far. In [6] the problem was superficially approached in the signal processing framework without thorough research. The system, shown in Fig. 2 is capable of electronic beam steering of generated wave both in elevation and azimuth. Perspective application of such a device may be in 3-D ultrasound imaging systems. The wave

Y. Tasinkevych is with the Department of Ultrasound, Institute of Fundamental Technological Research of the Polish Academy of Sciences, Warsaw, Poland (e-mail: yurijtas@ippt.gov.pl).

This work was supported by the Polish Ministry of Science and Higher Education (Grant NO. N515 500540).

Open Science Index, Biomedical and Biological Engineering Vol:7, No:11, 2013 publications.waset.org/17328/pdf

beam control is achieved by addressable driving of the 2-D matrix transducer through proper voltage supply of electrodes on the opposite faces of the piezoelectric layer. In this paper a semi-analytical method of analysis of the considered transducer is proposed, which is a generalization of the well-known BIS-expansion method [8]. It was earlier exploited with great success in the theory of interdigital transducers of surface acoustic waves [9], theory of elastic wave scattering by cracks and certain advanced electrostatic problems [10].

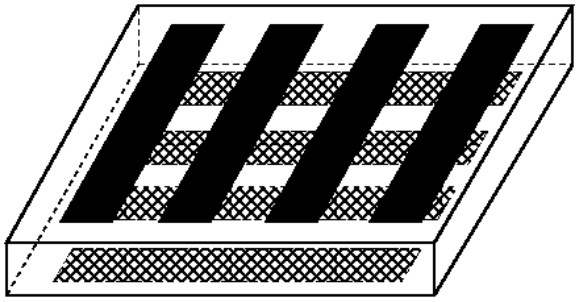


Fig. 2 System of crossed planar arrays of conducting strips arranged on the opposite faces of piezoelectric layer

Let's denote the driving signal applied to the upper and bottom strips as f_i and s_j, respectively, where i,j are the row and column numbers of the (i,j) matrix cell, located at the intersection of i^{th} upper and j^{th} bottom side strips. For the case of time-harmonic signals:

$$f_i = \cos\omega_i t,\ s_j = \cos(\omega_j + \Omega)t,\ \Omega \ll \omega_l,\ l = i,j, \tag{1}$$

the electric field and the resulting inducted normal stress will be localized near the $(i,j)^{\text{th}}$cell (especially for such piezoelectric materials like the PVDF [11]). In most applications the high frequency vibrations of the cells can be neglected. This yields the tool for selective (addressable) excitation of given cells: only this cell will vibrate with low frequency Ωwhich resides between strips driven by the signals f_i and s_j with frequencies differing by Ω. Thus, applying different amplitudes and phase-shifts to f_i, $s_j$or frequencies difference Ω, one obtains quite flexible tool for controlling vibrations of cells and the induced stress distribution over entire electrostrictive transducer matrix. The shape of vibrations requires detailed analysis of electric field distribution in the layer.

II. Spatial Spectrum of Planar Electric Field

To carry out the theoretical analysis the BIS-expansion method known from the theory of surface acoustic waves interdigital transducers [8] or electrostatics of planar periodic system of conducting strips [12] can be adopted with great success. Specifically, the electric field defined as$\mathbf{E}=-\nabla\varphi$, where $\varphi$is electrostatic potential, on the plane of strips can be expanded into the Bloch series as follows:

$$\begin{gathered} E = \{E_x, E_y\} = \sum_{n,m} E_{nm} \left\{\frac{r_n}{k_{nm}}, \frac{s_m}{k_{nm}}\right\} e^{-j(r_n x + s_m y)}, \\ r_n = r + nK,\ \ s_m = s + mK,\ \ k_{nm} = \sqrt{r_n^2 + s_m^2}, \end{gathered} \tag{2}$$

where $K = 2\pi/\Lambda$is a wavenumber of the strip array; Λ - is the strip period; $r \in (0,K)$ and $s \in (0,K)$ are arbitrary spatial spectrum variables reduced to one Brillouin zone for the uniqueness of representation. In (2) E_{nm} can be viewed as the amplitude of the plane harmonic field varying along the axis u rotated by the angle θ with respect to the x axis in the xy-plane:

$$\begin{gathered} E(u) = E_x \cos\theta + E_y \sin\theta = E_{nm} e^{-jk_{nm}u}, \\ \tan\theta = \frac{s_m}{r_n}. \end{gathered} \tag{3}$$

In the above equation E_x and $E_y$denote the components of the electric field corresponding to the $(n,m)^{\text{th}}$ spatial harmonic. The electrostatic potential appropriate to the (2) can be represented by the following expansion on the plane of strips:

$$\varphi = \sum_{n,m} \frac{E_{nm}}{k_{nm}} e^{-j(r_n x + s_m y)}. \tag{4}$$

It should be noted that generally, the tangential component of the electric field on the plane of strips depends on both the x and y spatial coordinates. This is achieved by using a strip model assuming that each strip is a stack of lateral sub-strips, so that the strip potential can vary between sub-strips (but it is constant on the sub-strips). The more detailed discussion can be found for instance in [13]. The normal component of electric induction $D \equiv D_z$ (whose jump discontinuity on the strips plane defines a surface electric charge) can be expanded into a similar series of spatial harmonics as in (2) but with corresponding amplitudes D_{nm}. The boundary conditions on the upper (superscript u) and bottom (superscript b) surfaces of the dielectric layer imposed on the field components are:

$$\begin{gathered} E_x^u = 0,\ \ E_y^b = 0,\ \ \text{on strips}, \\ D^u = 0,\ \ D^b = 0,\ \ \text{between strips}. \end{gathered} \tag{5}$$

Applying the BIS-expansion the surface fields components satisfying the boundary conditions given by (5) can be expressed in the following manner [14]:

$$\begin{gathered} E_x^u = \sum_{n',n,m} \alpha_{n'}^m S_{n-n'} P_{n-n'}(\cos\Delta) e^{-j(r_n x + s_m y)}, \\ D^u = \sum_{n',n,m} \tilde{\alpha}_{n'}^m P_{n-n'}(\cos\Delta) e^{-j(r_n x + s_m y)}, \\ E_y^b = \sum_{m',n,m} \beta_{m'}^n S_{m-m'} P_{m-m'}(\cos\Delta) e^{-j(r_n x + s_m y)}, \\ D^b = \sum_{m',n,m} \tilde{\beta}_{m'}^n P_{m-m'}(\cos\Delta) e^{-j(r_n x + s_m y)}, \end{gathered} \tag{6}$$

where $\Delta = Kw/2$; $P_k(\cdot)$ is the Legendre polynomials; $S_\nu = 0$ for $\nu < 0$ and $S_\nu = 1$ otherwise; w is the strip's width. The unknown coefficients $\alpha_{n'}^m$, $\tilde{\alpha}_{n'}^m$ and $\beta_{m'}^n$, $\tilde{\beta}_{m'}^n$ can be evaluated using the relation between spatial spectra of the tangential electric field $E^{u,b}$ and normal electric induction $D^{u,b}$ on the upper and bottom surfaces of the dielectric layer, which governs the field inside the layer [14]:

Open Science Index, Biomedical and Biological Engineering Vol:7, No:11, 2013 publications.waset.org/17328/pdf

$$\begin{bmatrix} E^u \\ E^b \end{bmatrix} = \frac{S_k}{j\varepsilon(k)} \begin{bmatrix} \coth|k|d & -1/\sinh|k|d \\ 1/\sinh|k|d & -\coth|k|d \end{bmatrix} \begin{bmatrix} D^u \\ D^b \end{bmatrix}. \quad (7)$$

It should be noted that the dielectric permittivity of the layer in (7) depends on k, but the fundamental feature is that for large wave-number value it reaches its constant limit ε_e [8]. The above relation directly results from the solution of the Laplace equation $\Delta\phi = 0$ inside the dielectric layer, where the electric potential φ can be expressed in the following form:

$$\varphi(u,z) = \left[Ae^{-|k|z} + Be^{|k|z}\right]e^{-jkz}, \ |z| < d/2. \quad (8)$$

In the above equation u is defined for the (n,m) component in (3). Evaluating the field components on the upper and bottom surfaces E_u, D_z:

$$E^{u,b} = E_u(\pm d/2), \ D^{u,b} = D_z(\pm d/2),$$

in the following way:

$$E^{u,b} = jk\left[Ae^{\mp|k|d/2} + Be^{\pm|k|d/2}\right]e^{-jku},$$
$$D^{u,b} = \varepsilon(k)|k|\left[Ae^{\mp|k|d/2} - Be^{\pm|k|d/2}\right]e^{-jku}, \quad (9)$$

and eliminating the constants A, B from the above one readily obtains (7). It is also worth noting, that the higher Bloch orders vanish fast inside the layer and are negligible on its opposite surface due to the term $1/(\sinh k_{nm}d)$. Thus, for large $k_{nm}$the corresponding spatial harmonics are well-localized at a given dielectric surface. This significantly simplifies the analysis due to the equations separation for large k_{nm}. The Bloch components from (6) must obey (9) for any numbers (n,m). Particularly, for (n,m) sufficiently large, such that:

$$\coth|k_{NM}|d = 1, \ \ 1/\sinh|k_{NM}|d = 0,$$

and $r_N/k_{NM} = 1$for the upper and $s_M/k_{NM} = 1$ for the bottom surface field representations, where N, M are some large but finite integers, the following approximation can be applied:

$$\tilde{\alpha}^m_{n'} = j\varepsilon_e\alpha^m_{n'}, \ \ \tilde{\beta}^n_{m'} = j\varepsilon_e\beta^n_{m'}. \quad (10)$$

Substituting the above equation into (6) yields:

$$E^u_x = \sum_{n',n,m} \alpha^m_{n'} S_{n-n'} P_{n-n'}(\cos\Delta)e^{-j(r_n x + s_m y)},$$
$$D^u = j\varepsilon_e \sum_{n',n,m} \alpha^m_{n'} P_{n-n'}(\cos\Delta)e^{-j(r_n x + s_m y)},$$
$$E^b_y = \sum_{m',n,m} \beta^n_{m'} S_{m-m'} P_{m-m'}(\cos\Delta)e^{-j(r_n x + s_m y)}, \quad (11)$$
$$D^b = j\varepsilon_e \sum_{m',n,m} \beta^n_{m'} P_{m-m'}(\cos\Delta)e^{-j(r_n x + s_m y)}.$$

Substitution of the Bloch components having the same wave-number k_{nm} from (11) into (7) for $n \in [-N,N]$, $m \in [-M,M]$ yields the system of linear equations for the unknown coefficients $\alpha^m_{n'}$ and $\beta^n_{m'}$, $n' \in [-N,N]$ and $m' \in [-M,M]$:

$$\alpha^m_{n'}\left[S_{n-n'}\tanh k_{nm}d - \frac{r_n}{k_{nm}}\right]P_{n-n'} -$$
$$\beta^n_{m'}\frac{r_n}{k_{nm}}\frac{P_{m-m'}}{\cosh k_{nm}d} = 0,$$
$$\alpha^m_{n'}\frac{s_m}{k_{nm}}\frac{P_{n-n'}}{\cosh k_{nm}d} + \quad (12)$$
$$\beta^n_{m'}\left[S_{m-m'}\tanh k_{nm}d - \frac{s_m}{k_{nm}}\right]P_{m-m'} = 0.$$

In (12) $P_l = P_l(\cos\Delta)$is applied to shorten notation.Due to the conditions leading to the approximation in (10) the equations for $\alpha^m_{n'}$ and $\beta^n_{m'}$ given by (12) outside the limits $n \in [-N,N]$, $m \in [-M,M]$are satisfied directly, what can be checked by inspection. The number of equations in (12) can be further reduced for the considered case of $s = 0$exploiting the symmetry properties of the unknown coefficients $\beta^n_{m'}$. Namely, substituting the identities involving the Legendre polynomials:

$$P_{-1-\nu}(\cos\Delta) = P_\nu(\cos\Delta)$$
$$P_l(-\cos\Delta) = (-1)^l S_l P_l(\cos\Delta) \quad (13)$$

into (12) yields:

$$\beta^n_{m'}(r) = \beta^n_{1-m'}(r), \quad (14)$$

where the dependence of the coefficients on r is shown explicitly. Taking into account (14) the equations in (12) can be transformed for $0 \le m, m' \le M$, with $-N \le n, n' \le N$ as follows:

$$\alpha^m_{n'}\left[S_{n-n'}\tanh k_{nm}d - \frac{r_n}{k_{nm}}\right]P_{n-n'} -$$
$$\beta^n_{m'}\frac{r_n}{k_{nm}}\frac{P_{m-m'} - P_{-m-m'}}{\cosh k_{nm}d} = 0,$$
$$\alpha^m_{n'}\frac{s_m}{k_{nm}}\frac{P_{n-n'}}{\cosh k_{nm}d} + \quad (15)$$
$$\beta^n_{m'}\sum_{l=-m,m}\left[S_{l-m'}\tanh k_{nm}d - \frac{s_m}{k_{nm}}\right]P_{l-m'} = 0.$$

In (15) the last equation for $m = 0$should be replaced with the following:

$$\frac{P_{n-n'}}{2\cosh kd}\alpha^0_{n'} -$$
$$\left[(-1)^{m'}\frac{k}{K}\tanh kd\frac{d}{d\xi}P_{-m'+\xi}\Big|_{\xi=0} - P_{-m'}\right]\beta^n_{m'} = 0, \quad (16)$$

where$k = k_{n0}$. The truncation numbers M, N involved in the system of linear equations, (15) and (16), generally should be

Open Science Index, Biomedical and Biological Engineering Vol:7, No:11, 2013 publications.waset.org/17328/pdf

infinite, but practically it is sufficient to apply N, Mnot very large finite integers. More specifically, let N', M' be such that:

$$\tanh N'Kd \approx \tanh M'Kd \approx 1, \quad (17)$$

Then $N > N'$ and $M > M'$ should be chosen such that $r_N/k_{NM'} \approx 1$ and $s_M/k_{N'M} \approx 1$, respectively (see (10) and the foregoing discussion). Integrating corresponding tangential components of the electric field one obtains the potential distribution on the plane of strips on the upper and bottom sides (which assumed to be given in the considered boundary-value problem as additional constrains to determine unknown expansion coefficients uniquely). For example, when a unitary voltage is applied to the l^{th} upper strip and all the bottom strips assumed to be grounded ($s = 0, s_m = mK$ in this case) this condition results in:

$$(-1)^{n'}\alpha_{n'}^{m}P_{-n'-r/K}(-\cos\Delta) = \delta_{m0}\frac{K}{\pi}e^{jrl\Lambda}\sin\pi r/K, \quad (18)$$

whereδ_{ij} - is the Kronecker delta. Solving (15), (16) and (18) for $\alpha_{n'}^{m}$ and $\beta_{m'}^{n}$, the planar electric field can be determined on both surfaces of the layer from (11).

III. Spatial Distribution of Electrostatic Field: Numerical Examples

Few numerical examples of electrostatic field distribution in the layer or, more exactly, its z-component, which results in the induced normal stress being the function of primary importance in applications, are presented below in this section. It is known [15] that the electric field is singular at the strip edges. Therefore, in order to avoid the corresponding difficulty, the z component of electric field at the layer middle plane $z = 0$ is evaluated. Specifically, for convenience, without loss of generality, the numerical examples of the normal induction $D_z$are shown below. It can be reconstructed from the surface normal induction D_z on both surfaces of the layer given by (11). In general case the electric field representation on both surfaces of the layer, (11), are defined for any $\rho = r + nK$ and $\tau = s + mK$, being the spectral variables corresponding to the x and y spatial coordinates. Therefore, (11) can be considered as the 2-D Fourier transforms of the corresponding spatial distributions of the electric field components on the planes of strips. Thus, using the spatial spectra of the normal induction on the upper D^u and bottom D^b faces of the layer,

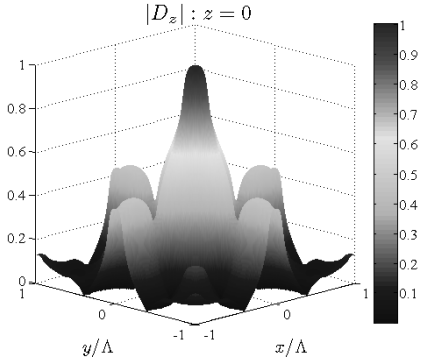
Equation (11), the normal induction on the plane $z = 0$, resulting directly from (9) (the constants A, B being expressed in terms of D^u, D^b), is:

$$D_z = \frac{D^u + D^b}{2\cosh|k|d/2}, \; k = k_{nm} = \sqrt{\rho^2 + \tau^2}. \quad (19)$$

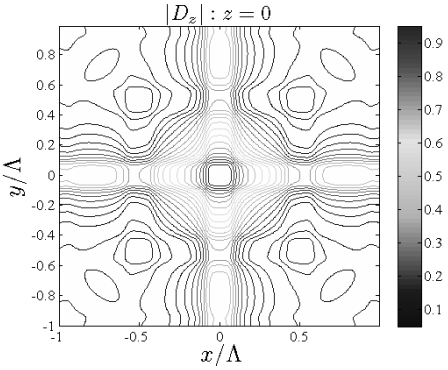
In the particular case considered here ($s = 0$) the function in (19) is defined in the spectral domain of continuous variable $\rho = r + nK$ and discrete $\tau = mK$ and the corresponding spatial counterpart can be found by the inverse 2-D Fourier transform as follows:

$$D_z(x,y) = \frac{2j}{K}\int_{-\infty}^{\infty} e^{-j\rho x} \times \sum_{m=-\infty}^{\infty} \frac{\alpha_{n'}^{m}P_{n-n'}(\cos\Delta) - \beta_{m'}^{n}P_{m-m'}(\cos\Delta)}{\cosh k_{nm}d/2} e^{-jmKy}. \quad (20)$$

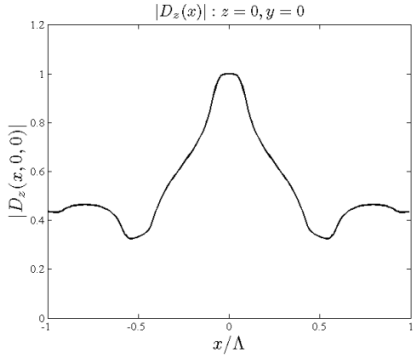
Fast growing term $1/(\cosh k_{nm}\, d/2)$ makes the above equation suitable for numerical evaluation. In Figs. 3 and 4 the numerical example of the D_z component of the electrostatic field in the layer middle plane $z = 0$ is shown in relative scale for fixed thickness of dielectric layer $d/\Lambda = 0.5$ and different width of strips w.



(a)



(b)



(c)

Fig. 3 The magnitude of the normal electric induction in the $\Lambda \times \Lambda$domainof the dielectric layer at the plane z=0 for $w/\Lambda = 0.15$ and plate thickness$d/\Lambda = 0.5$

Open Science Index, Biomedical and Biological Engineering Vol:7, No:11, 2013 publications.waset.org/17328/pdf

The example corresponds to the case when a single cell of the transducer is excited by uniform voltage applied to one upper strip and all bottom strips grounded. As is seen from Figs. 3, 4, the electric field distribution at the middle plane of the dielectric layer significantly departs from uniform and spans somewhat outside the cell covered by the supplied strips.

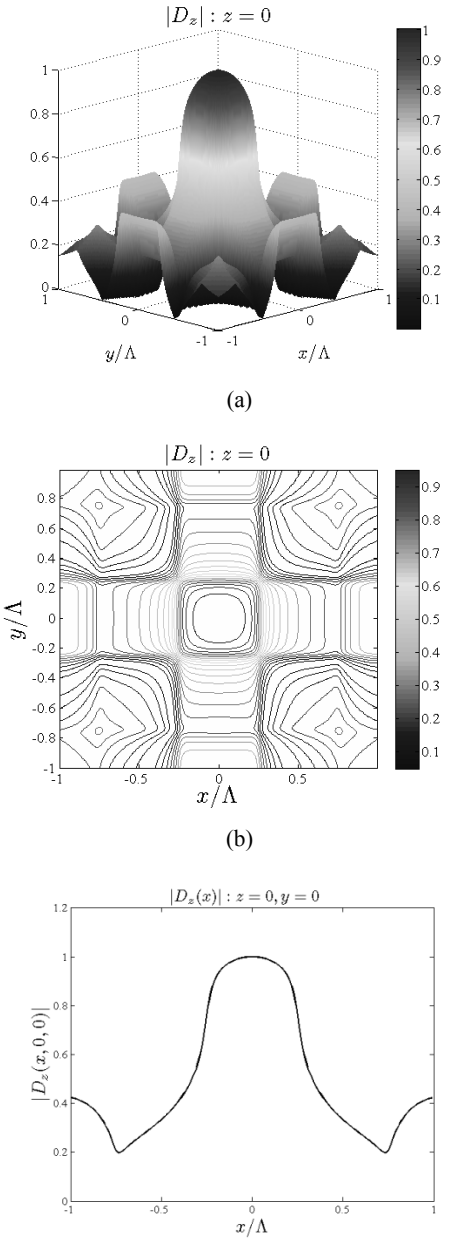


Fig. 4 The magnitude of the normal electric induction in the $\Lambda \times \Lambda$domainof the dielectric layer at the plane z=0 for $w/\Lambda = 0.5$ and plate thickness$d/\Lambda = 0.5$

IV. Conclusion

Summarizing, the extension of the BIS-expansion method, originally developed for electrostatic analysis of 1-D periodic planar systems of strips, was presented for modeling of 2-D periodic structure comprised of crossed arrays of strips placed on the opposite surfaces of the dielectric piezoelectric layer. It is an example of novel 2-D array transducer architecture with potential application in 3-D ultrasound imaging. Without loss of generality the same strip width an period on the opposite surfaces was assumed. The method can be generalized for different strip period and width straightforwardly. Numerical examples show the resulting nonuniform electrostatic field induced in the area of a single matrix cell excited by a uniform voltage applied to one upper strip and all bottom strips grounded.

References

[1] S. W. Smith, H. G. Pavy Jr., and O. T. von Ramm, "High-speed ultrasound volumetric imaging system. I. Transducer design and beam steering," *IEEE Trans.Ultrason., Ferroelectr. Freq. Contr*., vol. 38, no. 2, pp. 100-108, 1991.

[2] J. W. Hunt, M. Arditi, and F. S. Foster, "Ultrasound transducers for pulse-echo medical imaging," *IEEE Trans. Biomedical Eng*., no.8 pp. 453-481, 1983.

[3] P. C. Eccardt, K. Niederer, and B. Fischer, "Micromachined transducers for ultrasound applications," in *Proc. 1997 IEEE Ultrason. Symp*., vol. 2, pp. 1609-1618, 1997.

[4] E. D. Light, J. O. Fiering, P. A. Hultman, W. Lee, and S. W. Smith, "Update of two dimensional arrays for real time volumetric and real time intracardiac imaging," in *Proc. 1999 IEEE Ultrason. Symp*., vol. 2, pp. 1217-1220, 1999.

[5] S. W. Smith, W. Lee, E. D. Light, J. T. Yen, P. Wolf, and S. Idriss, "Two dimensional arrays for 3-D ultrasound imaging," in *Proc. 2002 IEEE Ultrason. Symp.*, vol. 2, pp.1545-1553, 2002.

[6] C. E. Morton and G. R. Lockwood, "Theoretical assessment of a crossed electrode 2-D array for 3-D imaging," in *Proc. 2003 IEEE Ultrason. Symp.*, pp. 968-971, 2003.

[7] C. H. Seo and J. T. Yen, "256x256 2-D array transducer with row-column addressing for 3-D imaging," in *Proc. 2007 IEEE Ultrason. Symp.*, pp. 2381-2384, 2007.

[8] K. Bløtekjær, K. A. Ingebrigtsen, and H. Skeie,"A method for analyzing waves in structures consisting of metal strips on dispersive media,"*IEEE Trans. Electron. Device*, vol. 20, pp. 1133-1138,1973.

[9] E. J. Danicki, "Electrostatics of interdigital transducers," *IEEE Trans. Ultrason., Ferroelectr. Freq. Contr*., vol. 51, no. 4, pp. 444-452, 2004.

[10] E. J. Danicki and Y. Tasinkevych, "Nonstandard electrostatic problem for strips," *J. Electrostatics*, vol. 64, no. 6, pp. 386-391, 2006.

[11] S. J. Jeong, C. H. Seo, and J. T. Yen, "Dual-layer transducer array for 3-D imaging," in *Proc. 2007 IEEE Ultrason. Symp.*, pp. 2371-2374, 2007.

[12] Y. Tasinkevych, Electrostatics: Theory and Applications. New-York: Nova Science Pub Inc., 2011, ch. Electrostatics of planar system of conducting strips, pp. 189-221.

[13] E. J. Danicki, "A method for analyzing periodic strips with apodization," *IEEETrans.Ultrason., Ferroelectr. Freq. Contr*., vol. 55, no. 9, pp. 1890-1894, 2008.

[14] E. J. Danicki, "Electrostatics of crossed arrays of strips," *IEEE Trans. Ultrason., Ferroelectr. Freq. Contr*., vol. 57, no. 7, pp. 1701-1705, 2010.

[15] O. P. Thakur and A. K. Singh, "Electrostriction and electromechanical coupling in elastic dielectrics at nanometricinterfaces," Material Science, vol. 27, p.839850, 2009.